Thermochimica Acta, 194 (1992) 77–85
Elsevier Science Publishers B.V., Amsterdam

Thermoanalysis as a tool for investigation of the formation of co-precipitated catalysts, with Fe-containing systems as an example

I.E. Nemirovskaya [1], A.N. Grechenko and A.M. Alekseev
State Institute of Nitrogen Industry (GIAP), ul. Chkalova, 50, 109815 Moscow (USSR)

(Received 29 March 1991)

Abstract

A series of studies have been made on the process of formation of catalytic systems based on ferric oxide using thermoanalysis methods, namely, differential scanning calorimetry, thermogravimetric analysis, X-ray diffraction analysis and dilatometry in static conditions in air atmosphere in non-isothermic conditions. The influence of the aluminium oxide content of the co-precipitated system on the course of the dehydration and crystallisation processes was also examined. The dynamics of the ferric oxide formation processes have been demonstrated. The activation energies of the different steps of the process have been calculated.

INTRODUCTION

Systems based on ferric oxides are used as catalysts for ammonia synthesis, CO shift conversion, ammonia oxidation, Fischer–Tropsch synthesis, etc. The process of preparation of such catalytic systems by means of co-precipitation depends on their intended use and includes several steps, of which the principal are co-precipitation from a mixture of solutions, thermal treatment of the hydroxides produced and reduction of the oxides.

The thermal treatment of crystalline systems is accompanied by a change in their structure and a redistribution of their defects. The final product of the thermal treatment is influenced, to a great extent, by the initial level of defects present which is determined by the nature of the crystals [1–8].

The theory of the crystallisation of slightly soluble hydroxides [9,10] shows that under the given conditions of oxide ageing, the direction of the phase transition is determined by the structure and chemical composition of the primary amorphous hydroxides.

A number of studies on the process of the preparation of iron-based catalysts have been published [1,9,11–17]. However, problems still exist,

[1] Author to whom correspondence should be addressed.

because either these studies do not cover to a necessary extent aspects of the formation of promotor catalysts, or else the physicochemical methods applied are not sufficiently informative to permit the full description of such systems. Thus, the application of new methods should reveal new, unknown regularities.

The aim of the present paper is to cover the following issues: the process of thermal treatment of co-precipitated ferric and aluminium hydroxides, the influence of aluminium oxide on the ferric oxide formation process and the reasons for this influence, and the process of ferric oxide crystallisation.

This paper reports the results of the analysis of the dynamics of the calcination process of the co-precipitated systems obtained (for the first time) in a set of thermoanalytical studies using programmed heating, and including such methods as differential scanning calorimetry (DSC), dilatometry (D), thermogravimetry (TGA) and also high-temperature X-ray analysis.

EXPERIMENTAL

The following systems were investigated: Fe_2O_3 and $Fe_2O_3 + xAl_2O_3$ ($x = 1$, 3, 5 and 8 wt.%).

The samples were prepared by means of co-precipitation of nitrate solutions by ammonia solution, and were then pre-calcinated to 413 K in air. The calorimetric studies were performed in the DSC 910 pressure system of a TA 990 instrument (DuPont, USA) at heating rates between 1 and 20 K min^{-1}, on finely dispersed powder samples (20–25 mg) in static air atmosphere or in a current of helium. If the heating rate is modified, the temperature of the thermoanalytical peak maximum will change [18]. In such a case the activation energy (E) may be determined according to the method of Kissinger (if it is assumed that at the peak temperature the fractional conversion is the same as at all heating rates used):

$$\Delta \ln(\lambda/T^2)/\Delta(1/T) = -E/R \qquad (1)$$

where λ is the heating rate (K min^{-1}), T the peak temperature (K) and R the gas constant.

From the slope of the graph of $\ln(\lambda/T^2)$ versus $1/T$, the activation energy, E (kJ mol^{-1}) can be determined.

The changes in the linear sides of sample tablets (diameter 9.42 mm, height 6–7 mm) were measured using an ED-408 dilatometer (Netsch, Germany) at a heating rate 5 K min^{-1} in static air atmosphere.

The change in phase composition of the samples was investigated by means of high-temperature X-ray diffraction in a Dron-2.0 (USSR) diffractometer with a GPVT-1500 high-temperature heater at the heating rate of about 5 K min^{-1} in static air atmosphere.

Thermogravimetric studies were carried out in a model 4433 ultramicrobalance (Sartorius, Germany) on samples of finely dispersed powder (20–25 mg) at a heating rate of 5 K min^{-1} in static air atmosphere.

RESULTS

Figure 1a shows the TGA curves for the amount of moles of water released (n) plotted against calcination temperature (T, K) in air for Fe_2O_3 (curve 1) and Fe_2O_3 + 8 wt.% Al_2O_3 (curve 4). Up to 380 K, only 1 mole of water has been released, irrespective of the ferric oxide being calcinated (with or without promotor). At 630 K, the process of water desorption comes to an end, and no further changes in weight can be observed.

The DSC curves are shown in Fig. 1b using a common scale and with the change in thermal flux, dQ/dt, plotted against temperature T (K). The dehydration process is accompanied by a 2–3-stage endothermic effect, its maximum deviation corresponding to a temperature of 350 K at the rate of 5 K min^{-1}. The maximum peak temperature is independent of the aluminium oxide content in the sample.

According to the results of the X-ray analysis, the transition from amorphous to crystalline ferric oxide in the sample without aluminium oxide (Fig. 2a) starts at a temperature of 600 K with the appearence of the lines corresponding to Fe_2O_3 phase (d = 2.69, 2.51, 1.84, 1.69, 1.485, 1.452 Å). At higher temperatures, the intensity of these lines increases. No lines corresponding to other phases could be detected in the X-ray diffraction pattern. The structure becomes stable at 700 K. The addition of aluminium oxide (e.g. 5 wt.%, Fig. 2b) shifts the temperature for the start of the transition up to 700 K. According to the results of the X-ray analysis, the solid-phase reaction between the co-precipitated oxides was not detected.

The process of crystallisation of that ferric oxide is accompanied by a two-stage exothermic effect (Fig. 1b). The maximum temperature of the most intense peak is increased from 640 to 780 K, together with an increase in the aluminium oxide content from 0 to 8 wt.% (heating rate 5 K min^{-1}).

The substitution of helium as the gaseous medium (purified by passage through activated coal and then zeolite 4A cooled to liquid nitrogen temperature) led to an increase in the intensity of the effects caused by the difference in the heat conductivity of helium and air. After-oxidation of the system does not take place while calcinating in air.

A change in the linear dimensions of the samples takes place during the process of calcination and consists of several stages (Fig. 1b). During the dehydration process (up to 570 K), the aluminium oxide content has no influence on the change in dimensions. A sharp decrease in the length of the sides takes place during the process of ferric oxide crystallisation. The increase in aluminium oxide content from 0 to 8 wt.% leads to an increase in the temperature of the start of the transition from 570 to 800 K. The

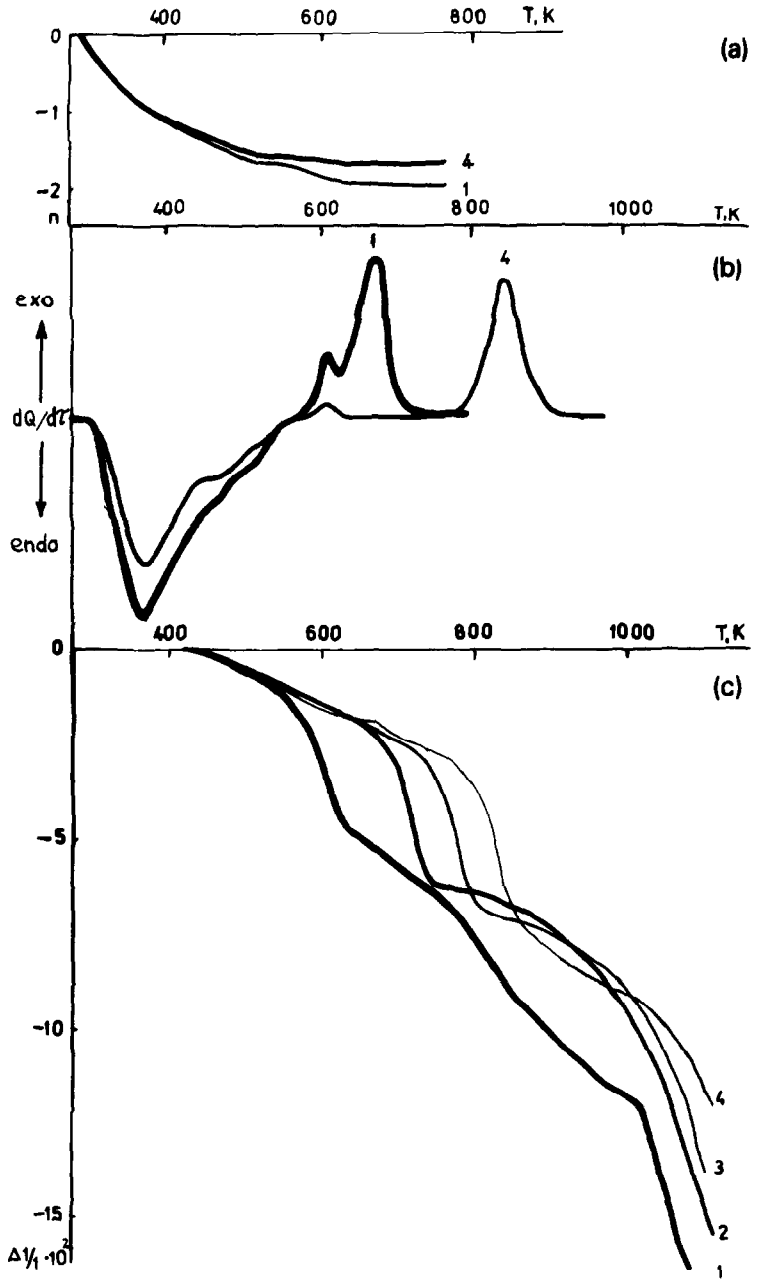

Fig. 1. The calcination of co-precipitated systems $Fe_2O_3 \cdot H_2O - xAl_2O_3$: $x = 0$ wt.%, curve 1; 3 wt.%, curve 2; 5 wt.%, curve 3; and 8 wt.%, curve 4; a, thermogravimetric curves; b, DSC curves; and c dilatograms.

total decrease in the dimensions of the sides in the course of the dehydration and crystallisation processes is linearly dependent on the aluminium oxide content: the change for non-promoted ferric oxide is 3.2% of the

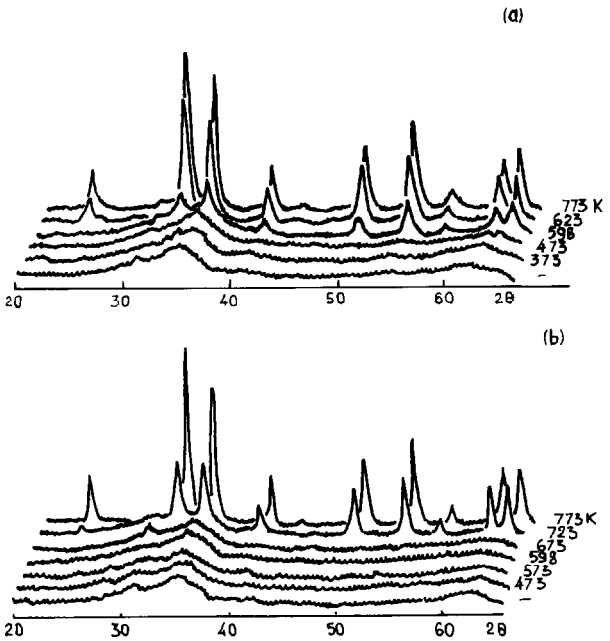

Fig. 2. XRD powder patterns of the systems: $Fe_2O_3 \cdot H_2O - xAl_2O_3$, where $x = 0$ wt.%, curve a, and 5 wt.%, curve b.

total side and this rises with increasing aluminium oxide content; at 8 wt.%, the decrease is 4.0% (see Fig. 3).

The nature of the changes that take place is identical for all the samples; the only difference lies in the temperatures of the transitions. At 760 K (e.g. for the sample with 3 wt.% Al_2O_3), there is a stabilisation of the sides; at 870 K, this stabilisation of the dimensions comes to an end. At temperatures higher than 1020 K, sintering of the samples starts, accompanied by a sharp decrease in the length of the sides. The increase in aluminium oxide content from 0 to 8 wt.% increases the temperature of sintering by 35 K. The introduction of only 3 wt.% aluminium oxide increases the stability of the system and its resistance to overheating.

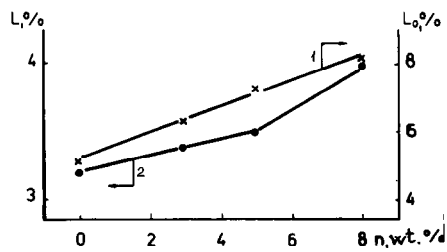

Fig. 3. Dependence of the sample size change on the content of aluminium oxide: 1, total (in the course of calcination); 2, in the course of dehydration.

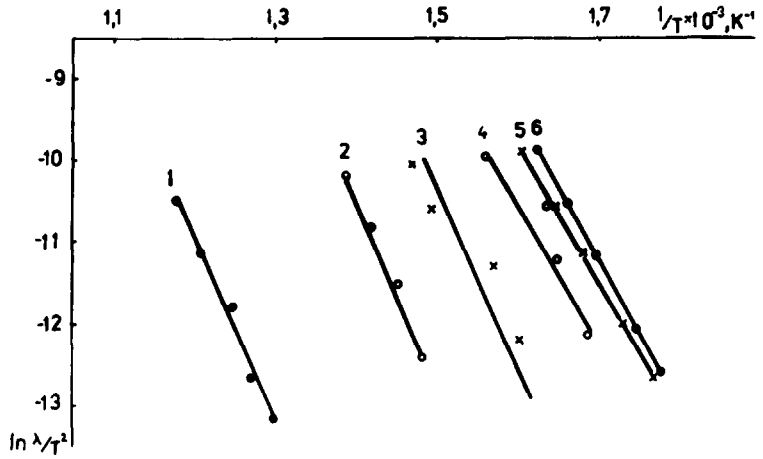

Fig. 4. Kinetic curves of the crystallisation processes of samples Fe_2O_3 (1, 2, 4, 6) and Fe_2O_3 + 8 wt.% Al_2O_3 (3, 5): 1–3, first stage; 4–6, second stage; atmosphere, air (1, 3, 5, 6); and He (2, 4).

The results of all the thermoanalytical methods are in agreement with each other.

DISCUSSION

The activation energy values for the dehydration of individual ferric hydroxide crystals in air and in helium are similar. The value of E for the first endothermic effect of the DSC curve is 42–50 kJ mol^{-1} which correlates with the thermal effect of water condensation (43.89 kJ mol^{-1} in refs. 19 and 20), see Fig. 4. Thus, the first stage of dehydration may be connected with non-structural water desorption. The region within which the endothermic effect emerges and the regions of weight loss and of decrease in linear dimensions, are located in the temperature range 300–400 K which correlates with published data [7,15,21–23]. However, whereas the quantity of water released must amount to 18.5–23.0 molecules per oxide molecule for the 5th day precipitate of ferric hydroxide (depending on the conditions of preparation) [21], for the samples under investigation, part of the non-structural water was desorbed during pre-calcination of the sample at 413 K.

Thus, in diluted mixed solutions of aluminium and ferric hydroxides, the polycondensation processes proceed continuously and are practically independent of each other, first by ferric hydroxide, and then by aluminium hydroxide. The polycondensation of each component in mixed solutions proceeds with the same intermediate products as in the individual solutions, as is confirmed by the results of ref. 10.

If in hydroxide systems the non-structural water content does not obey the rule of additivity, the chemical compounds formed in such a way will be of spinelide type; and the amount of water produced experimentally is less than that calculated theoretically. A number of systems of the following type do not obey this rule but form solid solutions with variable compositions: α-FeOOH–$Ce(OH)_3$ and $Mg(OH)_3$–β-$Co(OH)_2$–α-$Al(OH)_3$–α-FeOOH [19]. It is most probable that the system α-$Fe(OH)_3$–$Al(OH)_3$ belongs to this type of system.

The next stage is the removal of structural water. The amount of structural water does not depend on the precipitation conditions; according to refs. 19 and 20, in the case of ferric hydroxide, it corresponds to the phase composition of α-FeOOH. According to the results of different authors [7,19,24], the dehydration (decomposition) of α-FeOOH proceeds in the range between 410 and 620 K, is related to the difference in the conditions of preparation and examination of the samples, and is accompanied by an endothermic effect with activation energy value of about 75–112 kJ mol^{-1}, i.e. the relationship between the structurally bound water and the hydroxide base has the nature of an ionic interaction (the potential energy of an ionic bond amounts to 10^5 J mol^{-1} [4–6,22–26]). The number of water molecules per molecule of oxide is found to be 1.0. In the case of pure aluminium hydroxide, the quantity of water must amount to 2.0 water molecules per hydroxide molecule [19]; this corresponds to α-AlOOH. If the structural water content of hydroxide systems does not obey the rule of additivity, the interaction of the hydroxides is taking place.

The system under investigation is confirmed by the thermogravimetric data presented in Fig. 1a (curve 4). According to the DSC data, the activation energy of α-FeOOH decomposition amounts to 78 kJ mol^{-1} in helium atmosphere and increases up to 111 kJ mol^{-1} in air. At this stage of the process, the influence of the co-precipitated aluminium hydroxide manifests itself for the first time: it increases the activation energy value up to 166 kJ mol^{-1} (the temperature of the DSC peak maximum being increased by 20–30 K).

Thus, the temperature of the reaction increases from the first to the third stage of the dehydration. If the influence of the aluminium oxide in the ferric oxide does not manifest itself, at the first stage (desorption of non-structural water) at the final stage, when α-Fe_2O_3 is formed as a result of α-FeOOH decomposition, the co-precipitation components form a number of original "solid solutions" with variable composition and with complete reciprocal solubility of oxides.

The crystallisation of the amorphous hydroxides proceeds according to the mechanism of oriented growth [24]; the components exert reciprocal influences on each other which results in the change in the rates of crystallisation of the different components.

The process of calcination comes to an end with the crystallisation of

ferric oxide which occurs in two stages. The activation energy values for both stages confirm their independence of the gaseous medium in which the process takes place. The E value is about 120–150 kJ mol^{-1}, which is comparable with the typical values of crystallisation energy, e.g. the crystallisation of amorphous titanium [27]. The process of crystallisation is accompanied by nucleation of microcrystallites and their subsequent growth with temperature elevation. The influence of aluminium oxide becomes stronger in going from the first stage of crystallisation to the second stage: with the introduction of aluminium oxide, the temperature of the peak maximum increases by 5–10 K at the first stage, and by 160–170 K at the second stage. It seems impossible to form any conclusions concerning the stages of the crystallisation process from the results of the X-ray phase analysis (Fig. 2) because the crystallisation proceeds through nucleation of crystallites whose dimensions during the first stage are too small to be recorded, i.e. less than 20–30 Å. In this case, the calcination of co-precipitated aluminium and ferric hydroxides in both air and helium atmosphere does not lead to the appearance of a separate phase of iron–aluminium spinel (Fig. 2a, 2b). It seems that the presence of aluminium oxide can only be discerned by the changes in the lattice of the system which was formed during the calcination.

The calculation of the lattice parameters for samples with different aluminium oxide contents made it possible to observe the dependence of the lattice parameter on the aluminium content (Fig. 5). The dependence is linear for the samples calcinated to 770 K. In the range of investigated concentrations of aluminium oxide in ferric oxide, the constant value for the lattice parameter, i.e. the concentration limit of solubility of Al_2O_3 in α-Fe_2O_3, is not reached.

Thus, the data presented in this paper make it possible to observe all the stages of formation of oxide catalyst systems.

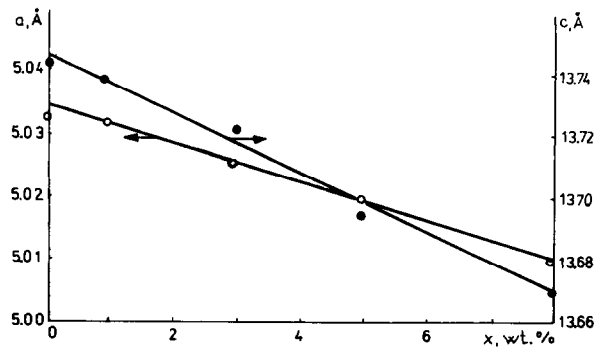

Fig. 5. Dependence of lattice parameters a and c of the system Fe_2O_3–xAl_2O_3 on the content of aluminium oxide, x.

ACKNOWLEDGEMENT

The authors thank Dr. L.A. Rudnitzky for carrying out the dilatometric studies.

REFERENCES

1 J. Cornejo, Mater. Chem. Phys., 15 (1986) 369.
2 M. Simoneita, Nouv. J. Chim., 6 (1982) 6.
3 V.A. Kaganovskij and V.M. Chertov, Ukr. Khem. Z., 52 (1986) 151.
4 F.J. Micale, D. Kiernan and A.C. Zettlemeyer, J. Colloid Interface Sci., 105 (1985) 570.
5 C.J. Serna and J.E. Iglesias, J. Mater. Sci. Lett., 5 (1986) 901.
6 T. Yamaguchi and T. Takahashi, J. Am. Ceram. Soc., 65 (1982) 83.
7 J. Subrt, F. Hanousek, V. Zapleval and H. Stepankova, J. Mater. Sci., 17 (1982) 215.
8 S.V.S. Prasad and R.V. Sitakara, J. Mater. Sci., 19 (1984) 3266.
9 Y. Sasa, M. Uda and I. Toyoshima, J. Mater. Sci. Lett., 5 (1986) 470.
10 O.P. Krivoruchko and R.P. Bujanov, Trudi Vses. skoli po katalizatoram, Part 3, Nauka, Novosibirsk, 1981, p. 122.
11 V.A. Dzisko, A.P. Karhauchov and D.V. Tarasova, Phyziko-chimicheskie osnovi sinteza okisnich katalizatorov, Nauka, Novosibirsk, 1978, p. 384.
12 D. Klissurski and I. Uzunov, Khim. Ind. Sofia, 55 (1983) 130.
13 I. Tadao, Calorim. Therm. Anal., 8 (1981) 71.
14 J. Fenerty, E. Hegarty and J. Pearck, Proc. 2nd Eur. Symp. Therm. Anal., Aberdeen, 1981, p. 395.
15 R.F. Menezes, V.N. Kamat Dalal and H.V. Keer, Proc. Indian Acad. Sci. (Chem. Sci.), 89 (1980) 247.
16 D.G. Klissurski, I.G. Mitov and K.P. Petrov, Thermochim. Acta, 181 (1980) 41.
17 A.V. Romenskii, I.V. Popik, V.I. Atroschenko and A.V. Lobojko, Izv. vuzov. Khem. Khem. Technol. (Russian high school reports. Chemistry and chemical technology) 28 (1985) 62.
18 N.P. Bansal and R.H. Doremus, J. Therm. Anal., 29 (1984) 115.
19 V.P. Chalij, Gidrokcidi Metallov, Naukova Dumka, Kiev, 1972, p. 152.
20 P. Staszczuk, Mater. Chem. Phys., 12 (1985) 111.
21 R.N. Tiwari, A.T. Balgopal and D.S. Chhabra, Fert. Technol., 21 (1984) 30.
22 V.S. Rao, S. Rajendran and H.S. Maiti, J. Mater. Sci., 19 (1984) 3593.
23 M. Rabif and H. Balkees, Proc. Indian Acad. Sci. (Chem. Sci.), 96 (1986) 315.
24 F. Watari, J. Landuyt, J. Delavignette and S. Amelinck, J. Solid State Chem., 29 (1979) 137.
25 C. Morterra, C. Mirra and E. Borello, J. Chem. Soc. Chem. Commun., 14 (1983) 767.
26 S. Hirokawa, T. Naito and T. Yamaguchi, J. Colloid Interface Sci., 112 (1986) 268.
27 M.V. Šušik, Mater. Chem. Phys., 12 (1985) 99.